

Methods to restore the dynamics of carbon condensation during the detonation of high explosives

I A Rubtsov^{1,4}, K A Ten^{1,4}, E R Prueel^{1,4}, A O Kashkarov^{1,4},
S I Kremenko⁴, M S Voronin¹, L I Shekhtman^{2,4}, V V Zhulanov^{2,4}
and B P Tolochko^{3,4}

¹ Lavrentyev Institute of Hydrodynamics of the Siberian Branch of the Russian Academy of Sciences, Lavrentyev Avenue 15, Novosibirsk 630090, Russia

² Budker Institute of Nuclear Physics of the Siberian Branch of the Russian Academy of Sciences, Lavrentyev Avenue 11, Novosibirsk 630090, Russia

³ Institute of Solid State Chemistry and Mechanochemistry of the Siberian Branch of the Russian Academy of Sciences, Kutateladze 18, Novosibirsk 630128, Russia

⁴ Novosibirsk State University, Pirogova Street 2, Novosibirsk 630090, Russia

E-mail: rubtsov@hydro.nsc.ru

Abstract. Time resolved small angle x-ray scattering (SAXS) experiments on detonating high explosives have been conducted at Lavrentyev Institute of Hydrodynamics and Budker Institute of Nuclear Physics. The purpose of these experiments is to measure the SAXS patterns behind the detonation front and restore the dynamics of a carbon condensation process. The deficiency of the experimental data hinders the development of detonation models. In this work we present a new method to restore the dynamic of carbon condensation from time resolved SAXS patterns.

1. Introduction

In the early 2000s, researchers from the Institute of Hydrodynamics, the Institute of Nuclear physics and the Institute of Solid State Chemistry and Mechanochemistry began to develop a new technique to study fast processes using high-energy accelerators [1]. The high intensity of synchrotron radiation (SR) allowed recording the dynamics of diffractive scattering with an exposure of 1 ns. In the first experiments on studying the process of carbon condensation, only integrated small angle x-ray scattering (SAXS) signal was possible to register. The SAXS intensity depends on electron density fluctuations due to carbon condensation in detonation of oxygen-deficient high explosives [1, 2]. Further development of equipment and methods of data processing led to obtain dynamics of the average size of the scattering centers in the Guinier approximation for various high explosives [3–5].

Similar station was put into operation at the Advanced Photon Source (APS, Argonne National Laboratory, United States) in 2015 [6]. These studies have shown hexanitrostilbene detonation produces carbon particles with a radius of gyration of 2.7 nm, which corresponds to the 7 nm diameter of spherical particles. It was recorded in 400 ns and remains constant for several microseconds. Further studies of larger charges (up to 2 g) [7–9] showed that the shape of SAXS patterns change and the carbon nanoparticles grows at least during the first 300 ns behind the detonation front. General description of the station and scheme of synchronization for

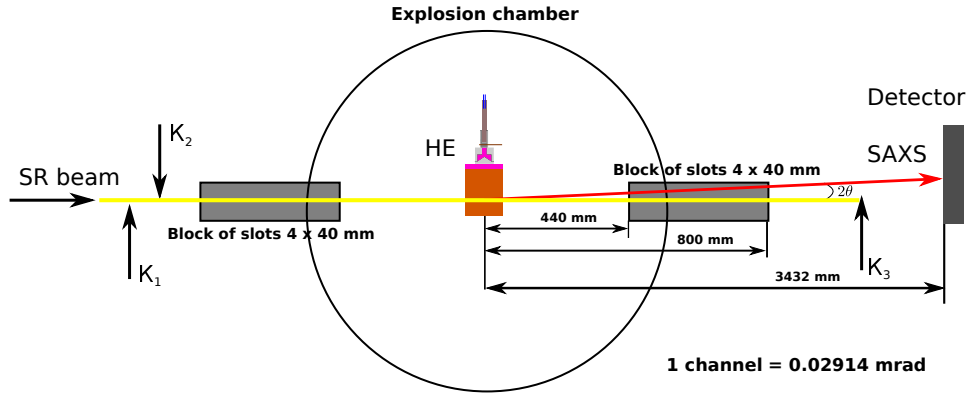


Figure 1. Experimental setup.

studying time resolved SAXS at the APS is presented in [10], the size of particles was recovered in Guinier approximation.

A series of works on the synthesis of ultradispersed diamonds by electromagnetic compression of graphite in thin copper tubes showed that all graphite passed into a diamond phase with a size of 5–25 nm [11, 12].

In this paper, we present new method of data interpretation on dynamic carbon condensation process. We take into account the expansion of the explosion products and the particle size distribution. The development of new methods of experimental data processing is necessary to confirm and improve the existing results on the dynamics of carbon condensation behind the detonation front.

2. SAXS measurement experiments

Time resolved SAXS measurements are carried out on the SYRAFEEMA (synchrotron radiation facility for exploring energetic materials) station which locates at the VEPP-4M beam line 8. The experimental setup is described in [13]. The SR beam was formed by high precision parallelepipeds K_1 and K_2 (no scattering Kratky SAXS collimator). The Kratky collimator was assembled ahead the explosion chamber. Straight beam was cut off by beam shield K_3 ahead the detector (figure 1). SAXS was recorded with a special gas DIMEX-3 detector with an angular resolution of 3×10^{-5} rad, located at 3432 mm from the explosive charge. The detector was filled with a mixture of Xe–CO₂ (75%–25%) at the pressure of 7 bar. The distance between detector channels is 0.1 mm. The used detector is capable of recording 100 frames every 124 ns [14].

The two-bunch mode of high-energy accelerator with a current of 10 mA and a bunch interval of 611 ns was used in experiment. The SR pulse duration was 73 ps [15]. To obtain SR beam 7-pole wiggler with a field of 1.3 T was used. The spectral characteristic of SR beam on SYRAFEEMA station (real spectrum) depends on a wiggler spectrum, and characteristics of chamber windows, charge and detector. The possibility of using such pink SR beam (figure 2) described in detail in [5].

Before the start of the experiment, the calibration measurements was made: attenuated primary beam, air scattering, scattering from the ultra-fine diamonds (UFD) (figure 3). First, a SR primary beam was formed by Kratky collimator with 1 mm in vertical size (~ 10 channels, curve 1). Then beam shield K_3 cut off the primary SR beam (curve 2). The amplitude of this signal corresponds to the scattering in the air and is taken as the zero signal. The experiments on SR scattering for UFD is extremely important to check the readiness of equipment for an experiment, evaluating the expected signal from explosives during the detonation, as well as to

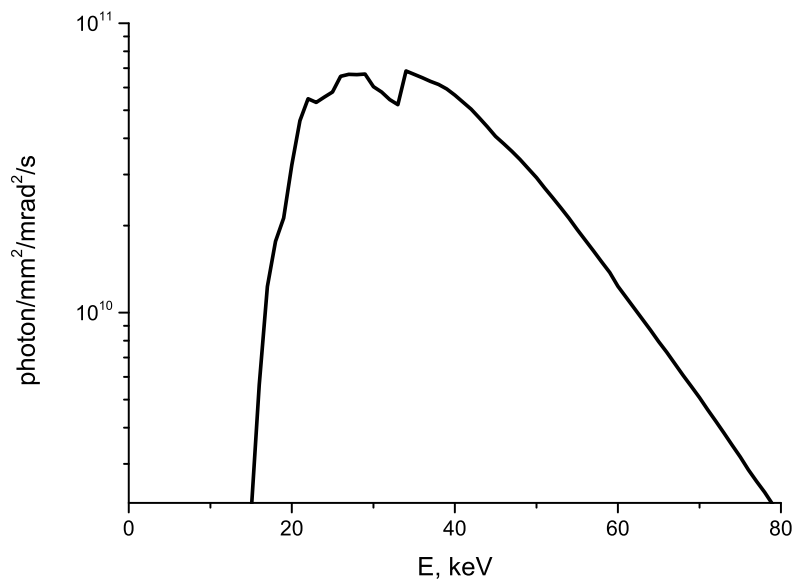


Figure 2. Real radiation spectral characteristic of the SYRAFEEMA station.

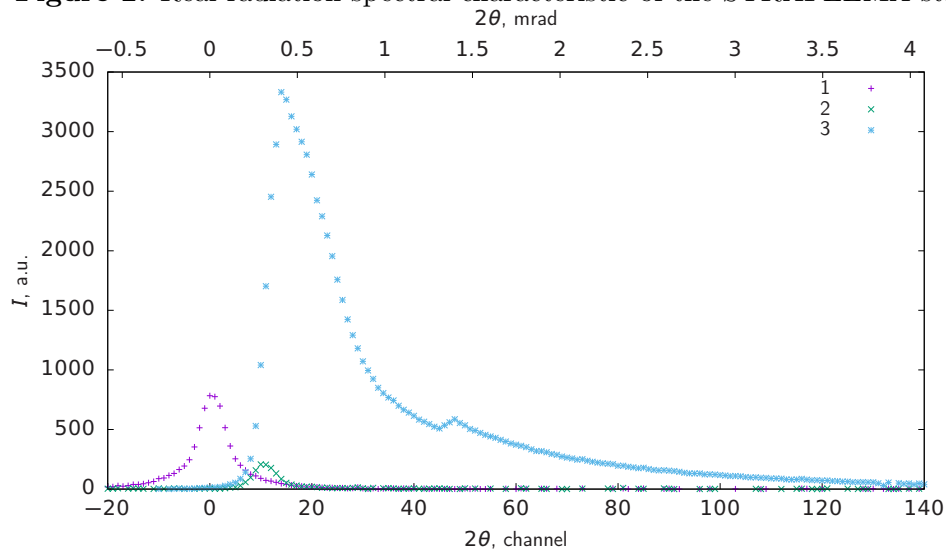


Figure 3. 1—attenuated primary beam; 2—air scattering, when primary beam blocked by beam shield K_3 ; 3—scattering from particles of UFD.

produce a SAXS calibration curve (curve 3).

3. Methods of restoring the dynamics of nanoparticles size from SAXS patterns

3.1. The expansion of detonation products

As the SR beam passes through the explosive charge, the part of the radiation is absorbed. The attenuation of the x-ray passing through a material (of density ρ and thickness d) is determined using the mass absorption coefficient μ/ρ which depends on the material. The intensity of the

attenuated radiation is given by the formula:

$$I = I_0 \exp\left(-\frac{\mu}{\rho}\rho d\right)$$

to find the time resolved real spectrum it is necessary to know the absorption of the sample (ρd), i.e. we should take into account the expansion of detonation products.

We calculate the expansion of the detonation products by using ANSYS Autodyn package and Jones–Wilkins–Lee equation of state for Composition B in cylindrical symmetry. The calculation results presented in figure 4. These distributions give us the ρd values obtained by integration along the radius at different time moments (figure 5).

Thus for each experimental frame, we obtain the value of ρd , real spectrum and its effective energy [5].

3.2. The Guinier method

Because of the SR beam has polychromatic spectrum, we introduce the concept of effective energy and wavelength for restoring SAXS data by Guinier method [5]. The SAXS intensity in Guinier approximation is defined by formula

$$I(q, R_g) = I_0 \exp\left(\frac{-q^2 R_g^2}{3}\right),$$

where R_g is the radius of gyration of the particle, $q = 4\pi \sin(\theta)/\lambda$ is the scattering vector, λ is the radiation wavelength and 2θ is the scattering angle. For a spherical homogeneous particle of radius R , the radius of gyration is $R_g = \sqrt{3/5}R$ [16, 17].

Taking the logarithm of the intensity

$$\ln(I(q, R)) = \ln(I_0) - \frac{q^2 R^2}{5},$$

we obtain a function which decreases linearly versus q^2 . From the slope k , of this plot we can determine the size of the spherical particle $D = 2R = 2\sqrt{5|k|}$ [16, 17].

Consideration of expansion of the detonation products allowed to use for each frame its own effective energy. The size of carbon nanoparticles restored from the static SAXS experiments for UFD (figure 3, curve 3) by Guinier method is presented in figure 6. The slope of the straight line approximation is $k \approx -7.7$, that corresponds to the scattering particles of the diameter of $D = 12.4$ nm.

3.3. SAXS multi diameter method

At the restoring data in Guinier approximation, we can receive only an average size of particles. To obtain the particle size distribution we implemented SAXS multi diameter (SMD) method. This method is to considered of the approximation of the experimental signal by superposition calculated SAXS signal from spherical particles of different diameters.

The intensity of SAXS signal from homogeneous spherical particles is defined by formula [16, 17]:

$$I(q, R) = \left(\frac{4}{3}\pi R^3\right)^2 \left[3 \frac{\sin(qR) - (qR) \cos(qR)}{(qR)^3}\right]^2. \quad (1)$$

Expressing in (1) q through the scattering angle 2θ and integrating over the spectrum, we obtain the dependence of the scattering intensity on the angle $I(2\theta, R)$.

Calculated SAXS signal $I_{\text{calc}}(2\theta)$ was computed by superposition of the obtained dependencies $I(2\theta, R)$:

$$I_{\text{calc}}(2\theta) = \sum_i N_i I(2\theta, R_i),$$

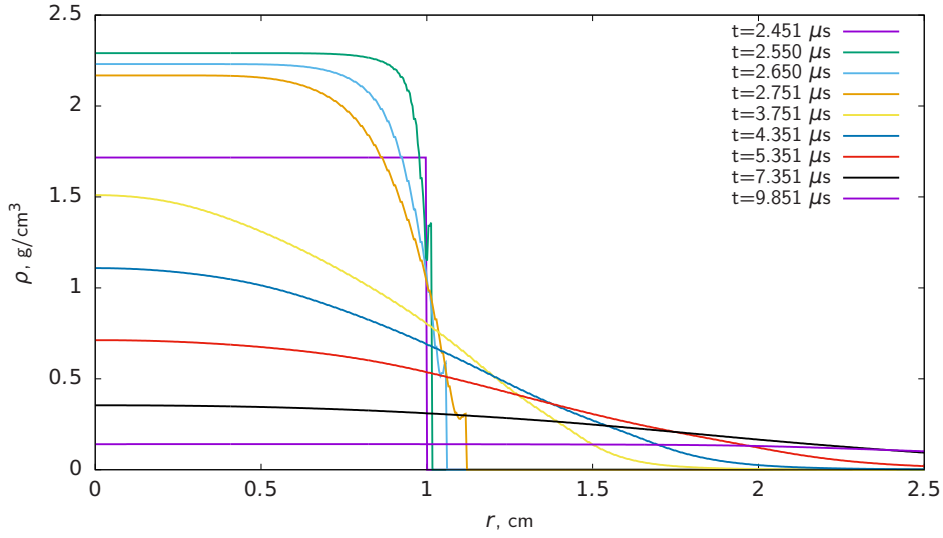


Figure 4. The dynamics of density distribution at the detonation of Composition B charge.

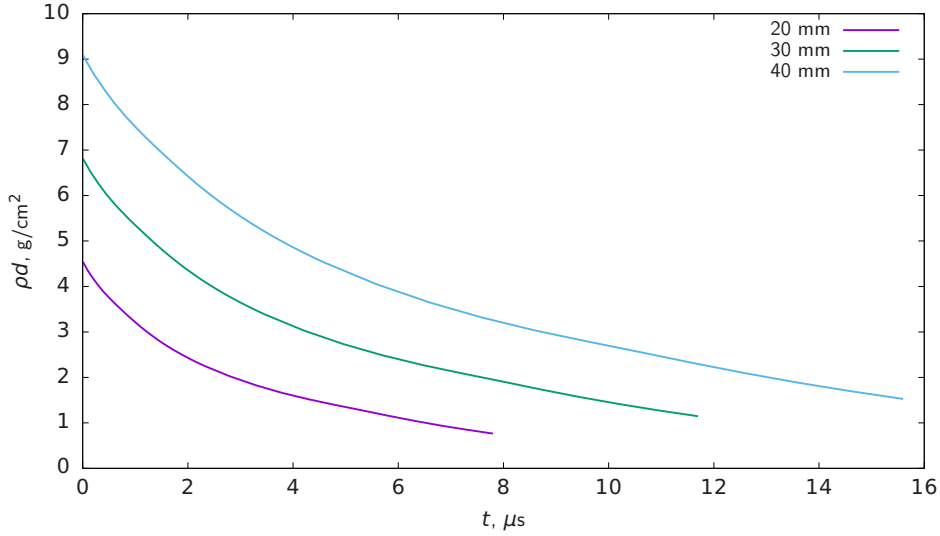


Figure 5. The dependences of ρd on time for charges with different diameter.

where N_i is the number of particles of the appropriate size in the scattering volume. To construct I_{calc} , the fixed set of particles with diameters from 1 to 200 nm was used.

The value of N_i were determined numerically from the condition of the best correspondence of the experimental and calculated SAXS signal. For this purpose, the minimum of the functional was sought:

$$\sum_j (I_{\text{exp}}(2\theta_j) - I_{\text{calc}}(2\theta_j))^2,$$

where $I_{\text{exp}}(2\theta_j)$ is the experimental SAXS signal, measured by detector.

The restored particle size distribution for UFD is shown in figure 7. The average size of the scattering centers in this method is defined as the arithmetic mean of the diameters with a

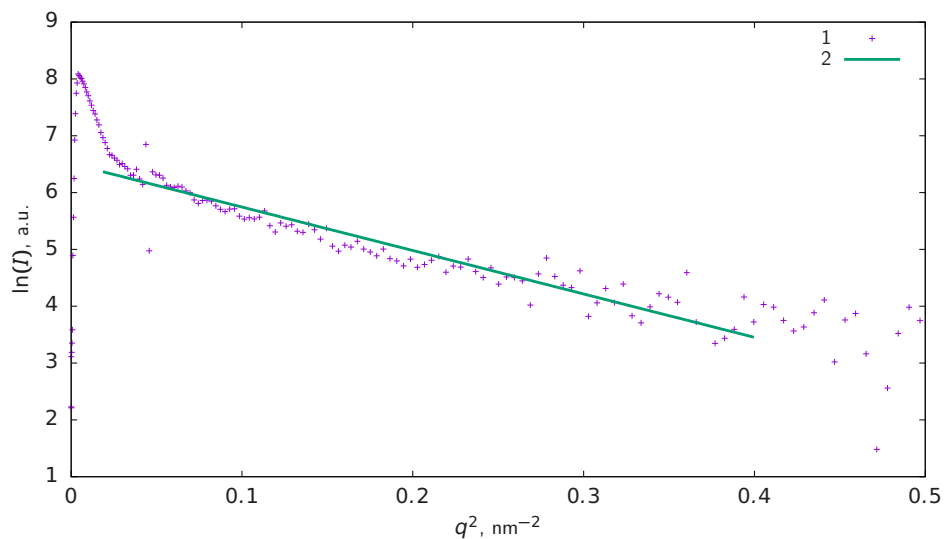


Figure 6. The dependences of $\ln(I)$ on q^2 : 1— $\ln(I)$; 2—approximation by straight line for UFD ($k \approx -7.7$, $D \approx 12.4$ nm).

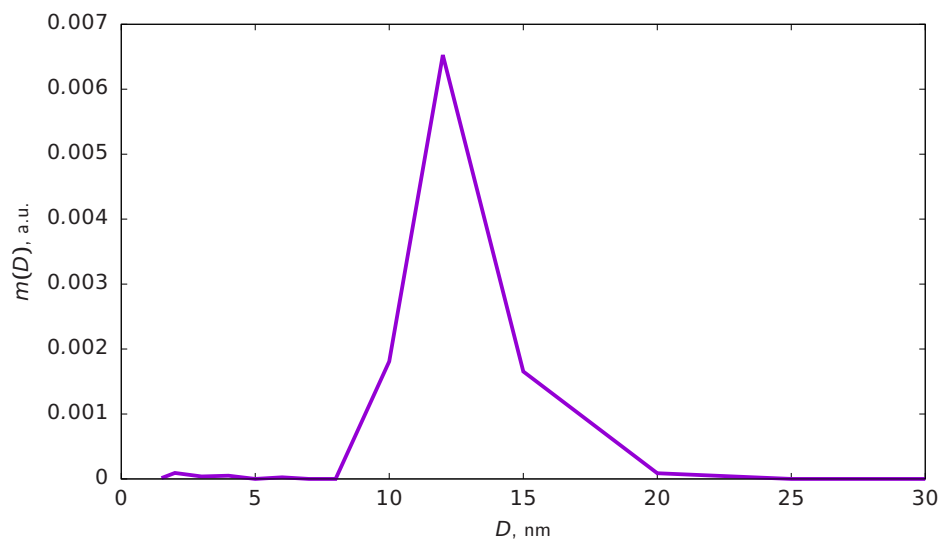


Figure 7. The particle size distribution for UFD (the volume fraction of particles with an appropriate diameter). $\langle D \rangle = 12.6$ nm.

weight of D^3 :

$$\langle D \rangle = \frac{\sum_i N_i D_i^3 D_i}{\sum_i N_i D_i^3}.$$

The particle size distribution of carbon nanoparticles restored from the static SAXS experiments on UFD (figure 3, curve 3) by SMD method is presented in figure 7. The average size of the scattering centers is equal to $\langle D \rangle = 12.6$ nm.

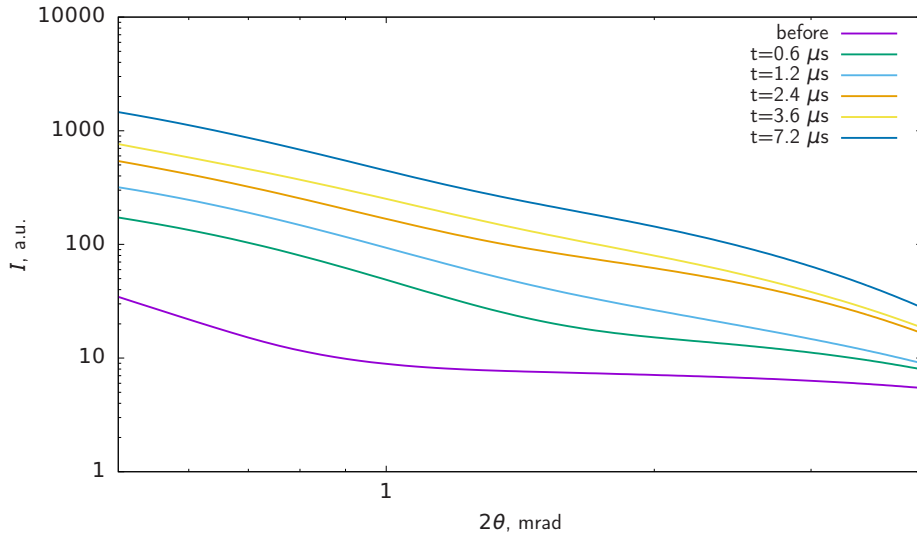


Figure 8. SAXS patterns during TNT–RDX detonation of 30 mm in diameter.

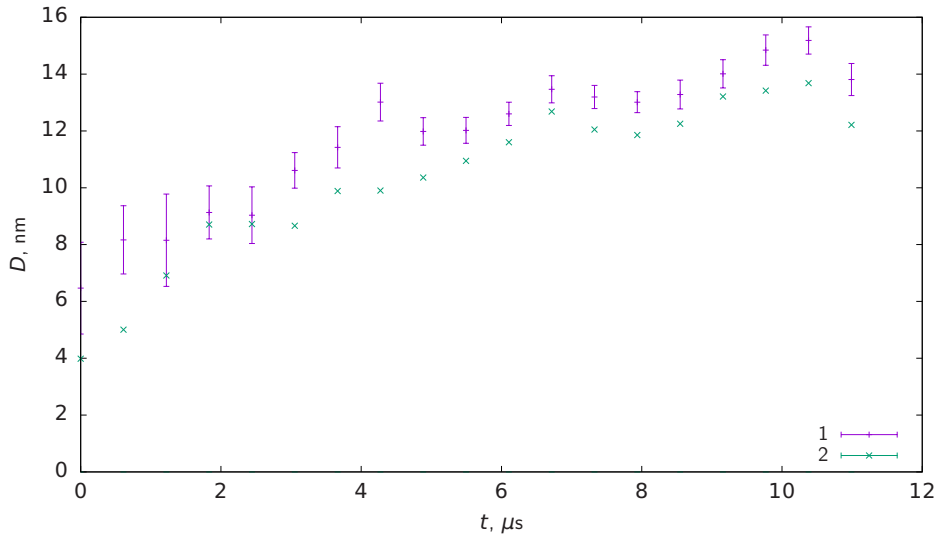


Figure 9. Average size of carbon particle versus time during TNT–RDX detonation of 30 mm in diameter: 1—from Guinier method; 2—from SMD method.

3.4. Comparison of the results of data interpretation

In static experiment, the methods were tested on the SAXS patterns from UFD (figure 3, curve 3). The results which presented in figures 6 and 7 show the size 12.4 and 12.6 nm for Guinier and SMD methods correspondingly. The recovered average size of particles exceeds the common size for UFD (4–7 nm) [18–20]. It was shown in [21] that size of UFD particles depends on method of investigation. The size, shape and morphology of condensed carbon nanoparticles from explosion products depends also on condition of the experiment [22].

In dynamic experiment, the methods were tested on the SAXS patterns during the detonation of TNT–RDX charge (figure 8). This results are shown in figure 9. It is seen that both methods are in a good agreement with each other. The late-time size is ≈ 13 nm, which confirms with

static experiment on UFD.

4. Conclusions

In this paper, the new SMD method for restoring the dynamics of average size of carbon nanoparticles from SAXS patterns was developed. The new method takes into account radiation spectrum and its changing during the detonation. It also allowed us to determine the particle size distribution. The SMD and Guinier methods are in a good agreement.

Acknowledgments

This work was supported by Russian Foundation for Basic Research (project No. 16-29-01050).

References

- [1] Aleshaev A N, Zubkov P I, Kulipanov G N, Luk'yanchikov L A, Lyakhov N Z, Mishnev S I, Ten K A, Titov V M, Tolochko B P, Fedotov M G and Sheromov M A 2001 *Combust., Explos. Shock Waves* **37** 585–93
- [2] Titov V M, Tolochko B P, Ten K A, Luk'yanchikov L A and Prueel E R 2007 *Diamond Relat. Mater.* **16** 2009–13
- [3] Ten K A, Prueel E R and Titov V M 2012 *Fullerenes, Nanotubes, Carbon Nanostruct.* **20** 587–93 (Preprint <https://doi.org/10.1080/1536383X.2012.656542>)
- [4] Ten K A, Titov V M, Prueel E R, Kashkarov A O, Tolochko B P, Aminov Yu A, Loboyko B G, Muzyrya A K and Smirnov E B 2014 Carbon condensation in detonation of high explosives *Proceedings Fifteenth International Detonation Symposium. Publication No. ONR-43-280-15* (San Francisco, CA) pp 369–74
- [5] Rubtsov I A, Ten K A, Prueel E R and Kashkarov A O 2016 *J. Phys.: Conf. Ser.* **774** 012071
- [6] Bagge-Hansen M, Lauderbach L, Hodgins R, Bastea S, Fried L, Jones A, van Buuren T, Hansen D, Benterou J, May C, Graber T, Jensen B J, Ilavsky J and Willey T M 2015 *J. Appl. Phys.* **117** 245902 (Preprint <https://doi.org/10.1063/1.4922866>)
- [7] Firestone M A, Dattelbaum D M, Podlesak D W, Gustavsen R L, Huber R C, Ringstrand B S, Watkins E B, Jensen B, Willey T, Lauderbach L, Hodgins R, Bagge-Hansen M, van Buuren T, Seifert S and Graber T 2017 *AIP Conf. Proc.* **1793** 030010 (Preprint <http://aip.scitation.org/doi/pdf/10.1063/1.4971468>)
- [8] Willey T M, Bagge-Hansen M, Lauderbach L, Hodgins R, Hansen D, May C, van Buuren T, Dattelbaum D M, Gustavsen R L, Watkins E B, Firestone M A, Jensen B J, Graber T, Bastea S and Fried L 2017 *AIP Conf. Proc.* **1793** 030012 (Preprint <http://aip.scitation.org/doi/pdf/10.1063/1.4971470>)
- [9] Watkins E B, Velizhanin K A, Dattelbaum D M, Gustavsen R L, Aslam T D, Podlesak D W, Huber R C, Firestone M A, Ringstrand B S, Willey T M, Bagge-Hansen M, Hodgins R, Lauderbach L, van Buuren T, Sinclair N, Rigg P A, Seifert S and Gog T 2017 *J. Phys. Chem. C* **121** 23129–40 (Preprint <http://dx.doi.org/10.1021/acs.jpcc.7b05637>)
- [10] Gustavsen R L, Dattelbaum D M, Watkins E B, Firestone M A, Podlesak D W, Jensen B J, Ringstrand B S, Huber R C, Mang J T, Johnson C E, Velizhanin K A, Willey T M, Hansen D W, May C M, Hodgins R L, Bagge-Hansen M, van Buuren A W, Lauderbach L M, Jones A C, Graber T J, Sinclair N, Seifert S and Gog T 2017 *J. Appl. Phys.* **121** 105902 (Preprint <https://doi.org/10.1063/1.4978036>)
- [11] Oreshkin V I, Chaikovskii S A, Labetskaya N A, Ivanov Y F, Khishchenko K V, Levashov P R, Kuskova N I and Rud' A D 2012 *Tech. Phys.* **57** 198–202
- [12] Melnikova N V, Alikin D O, Melnikov Y B, Grigorov I G, Chaikovskiy S A, Labetskaya N A, Datsko I M, Oreshkin V I, Ratakhin N A and Khishchenko K V 2016 *J. Phys.: Conf. Ser.* **774** 012012
- [13] Titov V M, Prueel E R, Ten K A, Luk'yanchikov L A, Merzhievskii L A, Tolochko B P, Zhulanov V V and Shekhtman L I 2011 *Combust., Explos. Shock Waves* **47** 615–26
- [14] Shekhtman L, Aulchenko V, Kudryavtsev V, Kutovenko V, Titov V, Zhulanov V, Prueel E, Ten K and Tolochko B 2016 *Phys. Procedia* **84** 189–96
- [15] Blinov V E, Bobrovnikov V S, Zolotarev K V, Kiselev V A, Kononov S A, Kurkin G Ya, Levichev E B, Meshkov O I, Muchnoi N Yu, Nikiti S A, Nikoilenko D M, Sukhanov D P, Tikhonov Yu A, Tolochko B P, Tumaikin G M, Shamov A G and Shatilov D N 2014 *Phys. Part. Nucl. Lett.* **11** 620–31
- [16] Feigin L A and Svergun D I 1987 *Structure Analysis by Small-Angle X-Ray and Neutron Scattering* (NY, Plenum Press.)
- [17] Schnablegger H and Singh Y 2013 *The SAXS Guide* (Anton Paar GmbH)
- [18] Greiner N R, Phillips D S, Johnson J D and Volk F 1988 *Nature* **333** 440–2
- [19] Volkov K V, Danilenko V V and Elin V I 1990 *Combust., Explos. Shock Waves* **26** 366–8
- [20] Pantea D, Brochu S, Thiboutot S, Ampleman G and Scholz G 2006 *Chemosphere* **65** 821–31

- [21] Kashkarov A O, Prueel E R, Ten K A, Rubtsov I A, Gerasimov E Yu and Zubkov P I 2016 *J. Phys.: Conf. Ser.* **774** 012072
- [22] Huber R C, Ringstrand B S, Dattelbaum D M, Gustavsen R L, Seifert S, Firestone M A and Podlesak D W 2018 *Carbon* **126** 289–98